

# Evaluating the critical velocity of air entrainment by plunging water jets

Yuri Fetisov<sup>1</sup>, Yuliya Bryanskaya<sup>2\*</sup>, and Evgenii Ignatenko<sup>2</sup>

<sup>1</sup>Volgograd State Technical University, Volgograd, 400005, Russia

<sup>2</sup>National research Moscow State University of Civil Engineering, Moscow, 129337, Russia

**Abstract.** It has been found that air entrainment occurs when the average jet velocity at the plunging point reaches a certain value. This velocity is called the critical velocity of air entrainment. The analysis of studies in this field shows that the process of jet interaction with the liquid surface is complex, while the theoretical approaches to its description are insufficient. The conditions at which air entrainment begins are related to the behavior and shape of the meniscus. The mechanism of meniscus formation is based on the complicated kinematic structure of motion in the vicinity of the point of interaction between the jet and the liquid in the quiescent state. Experiments and observations show that the meniscus behavior is closely related to the initial conditions of air entrainment. Calculating the critical velocity of air entrainment  $U_c$ , analysis of the meniscus shape, and use of the limit equilibrium condition were used to derive a new criterion relationship for the air entrainment conditions of turbulent jets flowing from long smooth nozzles. The results of calculations are compared with experimental data.

## 1 Introduction

The article attempts to evaluate the minimal velocity  $U_c$  at which a turbulent free jet starts entraining air when plunging into a liquid at rest.

When the falling jet meets the surface of the liquid at rest, the air is intensely entrained. The entrained air reduces the eroding capacity of a directed or free-falling jet at the interaction between the pools of hydroengineering structures. It decreases the cavitation erosion of structure elements [1,2]. The jet-induced aeration is used to saturate the water with oxygen from the air to improve its quality and intensify the biological treatment processes of wastewater. In other cases, aeration causes adverse effects [3-6] (e.g., steel, glass, and paint teeming). Therefore, this phenomenon manifests itself in many problems, which are of importance in some spheres of engineering and technology. It was found that air entrainment can occur under conditions when the average velocity of the jet at the entry into the liquid reaches a certain value. This velocity is referred to as the critical velocity of air entrainment.

Experiments show [7-9] that at small jet velocities, no air is entrained. In this case, the jet enters the receiving liquid as a rigid rod, as shown in the photo in Fig. 1. This photo

---

\* Corresponding author: [mgsu-hydraulic@yandex.ru](mailto:mgsu-hydraulic@yandex.ru)

shows that a meniscus forms at the jet entry into the liquid. This pattern of interaction between the jet and the liquid at rest has been described by A. Sheridan [10]. The conditions at which air entrainment begins are related to the behavior and shape of the meniscus. The analysis of publications referring to the subject of this study [9, 11-19] shows that the process of jet interaction with the liquid surface is complex. At the same time, the theoretical approaches to its description are underdeveloped.

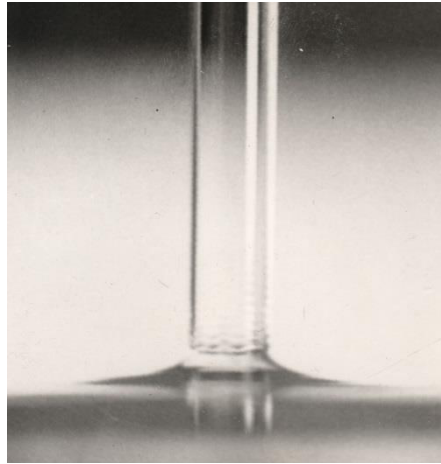


**Fig. 1.** The jet enters the receiving liquid as a rigid rod

The mechanism of meniscus formation is not clear. The literature gives neither data nor ideas about this.

## 2 Materials and Methods

When a jet plunges into a liquid at rest, a meniscus forms at the water-air interphase. The assumption that such an interaction pattern results from jet spreading at its meeting the horizon of the liquid at rest seems hardly reasonable. Indeed, when entering into the liquid, the jet plunges. According to the above researchers, the expansion angle of the such jet at the initial segment is  $8\div 14^\circ$ . The photo in Fig. 1 shows this angle to be about  $90^\circ$ . A similar pattern of jet spreading can be seen at its meets a solid surface.

The mechanism of meniscus formation seems to be based on the complicated kinematic motion structure in the vicinity of the point of interaction between the jet and the liquid at rest. When entering the liquid, the jet starts entraining the nearby layers due to friction forces at its lateral surface. The result is the formation of a circulation motion within the meniscus. The formation accompanies this process on the surface of the receiving liquid of velocity components directed along radiuses toward the jet's center. The velocity increases toward the jet because of the decrease in the cross-section of the radial flow. Because of this, the water level rises near the jet, similar to that observed when moving liquid meets a solid obstacle (a cylinder). The difference is that when a liquid meets a solid cylinder, a permanently collapsing roller forms with a shape of a collar. When the flow meets a jet, no such collapse occurs because the jet keeps entraining the liquid. In this case, the surface of interaction is similar to a sink. The resulting curvature of the free liquid surface creates surface tension forces at the gas-liquid interface. These forces keep the meniscus.

Experiments and observations of other researchers [10,11] show that the meniscus behavior is closely related to the initial conditions of air entrainment. An increase in jet

velocity causes a decrease in the height of the meniscus up to the moment when the meniscus disappears as if overturning. A funnel appears around the jet, and individual air bubbles appear in the liquid, demonstrating the start of the entrainment process. Therefore, air entrainment can be associated with the overturning of the meniscus and the effect of perturbations on the jet surface (Fig. 2b). After meniscus overturning, the amount of entrained air is related to the wave-like perturbations on the jet [7].

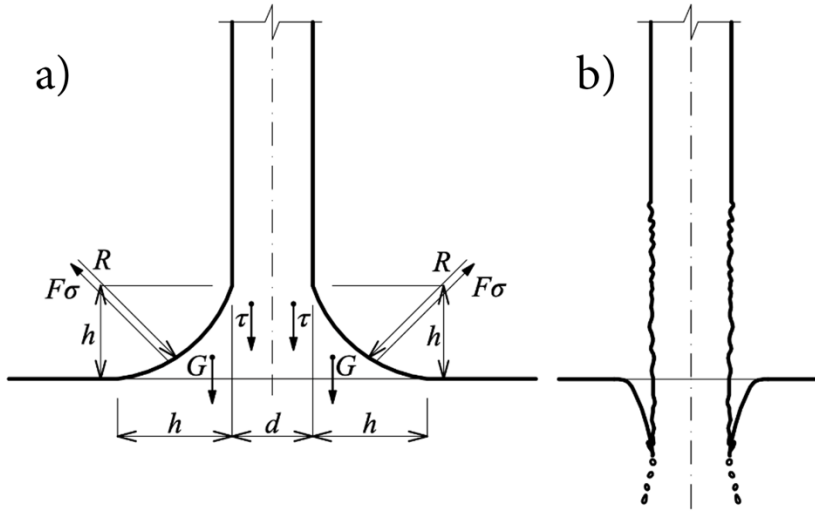


**Fig. 2.** Meniscus state: (a) no air entrainment; (b) air entrainment is taking place

To calculate the critical velocity of the start of air entrainment  $U_c$ , we consider the condition of limit equilibrium. In this state, the meniscus will be in equilibrium under the effect of the gravity force, surface tension force, and friction force at the lateral surface of the jet at the meniscus interface, as shown in Fig. 2a.

The equilibrium condition in projections on the vertical axis can be written as

$$F_\tau + G - F_{\sigma z} = 0 \tag{1}$$

where  $F_\tau$  is the friction force on the lateral surface of the jet;  $G$  is liquid weight within the meniscus;  $F_{\sigma z}$  is the vertical component of the surface tension force.

With denotations shown in Fig. 2, the friction force is

$$F_\tau = \pi d h \tau \tag{2}$$

where  $\tau$  is the tangential stress between the jet and the meniscus;  $h$  is meniscus height.

The meniscus volume can be evaluated with acceptable accuracy as the volume of a truncated cone with diameters of  $(d + 2h)$  and  $d$  minus the liquid volume in a cylinder with diameter  $d$ . The assumption that the width and height of the meniscus are equal to  $h$  is justified for the equilibrium conditions because of the homogeneity of liquids. Now, the weight of the liquid within the meniscus can be written as

$$G = \frac{1}{2} \rho g \pi d h^2 \left( 1 + \frac{2h}{3d} \right) \tag{3}$$

The vertical projection of the surface tension force can be derived from the relationship

$$F_{\sigma z} = p_{\sigma} S_k \quad (4)$$

where  $p_{\sigma}$  is capillary pressure;  $S_k$  is the horizontal projection of the curvilinear surface of the meniscus.

The capillary pressure can be found by the Laplace formula:

$$p_{\sigma} = \sigma \left( \frac{1}{R} + \frac{1}{r} \right) \quad (5)$$

where  $\sigma$  is surface tension coefficient;  $R$  is the radius of curvature of the meniscus;  $r$  is jet radius (radius of mutually perpendicular direction towards curvature radius  $R$ ).

As we search for the vertical component of the force  $F_{\sigma}$ , the capillary pressure is determined by the curvature  $R$ , i.e.,

$$p_{\sigma} = \frac{\sigma}{R} \quad (6)$$

The horizontal projection of the meniscus is a ring with an area of

$$S_k = \pi dh \left( 1 + \frac{h}{d} \right) \quad (7)$$

Considering (6) and (7), expression (4) becomes

$$F_{\sigma z} = \frac{\sigma}{R} \pi dh \left( 1 + \frac{h}{D} \right) \quad (8)$$

and the equilibrium condition (1), considering (2), (3), and (8), can be written as

$$\pi dh \tau + \frac{1}{2} \rho g \pi dh^2 \left( 1 + \frac{2h}{3d} \right) = \frac{\sigma}{R} \pi dh \left( 1 + \frac{h}{d} \right) \quad (9)$$

or, after reduction,

$$\tau + \frac{1}{2} \rho gh \left( 1 + \frac{2h}{3d} \right) = \frac{\sigma}{R} \left( 1 + \frac{h}{d} \right) \quad (10)$$

The latter relationship is the equilibrium condition of the meniscus in the limiting state, written with the acting forces taken into account.

Now, the solution requires the evaluation of the unknown variables in (10), i.e.,  $\tau$ ,  $h$ ,  $R$ . No experimental data have been found for the tangential friction stress at the initial segment of the jet at the interaction point.

Direct measurements on the photographs of menisci in the limiting state at  $h \rightarrow 0$  showed that  $\frac{R}{h} \cong 4$ .

This enables the estimation of the radius of curvature  $R$  with the assumption that the tangential stresses in the limiting state are negligible. Now the relationship (10) can be written as

$$\frac{1}{2}\rho gh\left(1+\frac{2h}{3d}\right)=\frac{\sigma}{R}\left(1+\frac{h}{d}\right), \quad (11)$$

Considering that  $\frac{R}{h}\cong 4$ , equation (11) can be used to find meniscus curvature radius

$$R=\sqrt{\frac{8\sigma}{\rho g}}\sqrt{\frac{1+\frac{h}{D}}{1+\frac{2h}{3d}}} \quad (12)$$

Clearly, at  $h\rightarrow 0$ , the value of the second square root in (12) is close to 1; therefore, the radius of curvature can be written as

$$R=\sqrt{\frac{8\sigma}{\rho g}} \quad (13)$$

With such assumptions, the radius of curvature of the meniscus will depend on the surface tension and liquid density.

We also assume that, under limiting equilibrium, the weight of the liquid determined by (3) is negligible, so expression (10) becomes

$$\tau=\frac{\sigma}{R}$$

At  $h\rightarrow 0$  and considering that  $\tau=C_f\rho\frac{U_e^2}{2}$ , where  $C_f$  is the specific friction resistance, this relationship can be written as

$$C_f\rho\frac{U_e^2}{2}=\frac{\sigma}{R} \quad (14)$$

Whence

$$U_e=\sqrt{\frac{2\sigma}{C_f\rho R}} \quad (15)$$

Considering (13), we have

$$U_e=\frac{0.84}{\sqrt{C_f}}4\sqrt{\frac{\sigma g}{\rho}} \quad (16)$$

Formula (16) gives a relationship for calculating the critical velocity of the start of air entrainment derived from the proposed formalization of the process. Formula (16) does not explicitly contain the geometric characteristics of the jet, nor does it contain the viscosity.

However, correlation (16) contains the friction coefficient  $C_f$ , depending on the Reynolds number. As noted above, evaluating the friction coefficient  $C_f$  for such conditions is very difficult.

We suppose that the structure of the jet does not change considerably during the time required for the liquid to move from the nozzle to the interaction point. Therefore, we can assume that the tangential stresses on jet lateral surface will be determined by the turbulent structure that has formed in the nozzle. In the conducted experimental studies [7], long smooth nozzles made of brass tubes were used. For such nozzles, hydraulic friction coefficient  $\lambda$  can be found from the Blasius formula

$$\lambda = \frac{0.3164}{\text{Re}^{0.25}} \quad (17)$$

The approximate relationship between  $\lambda$  and  $C_f$  has the form

$$C_f = \frac{\lambda}{4} \quad (18)$$

Considering (17), the frictional specific resistance for smooth pipes will be

$$C_f = \frac{0.079}{\text{Re}^{0.25}} \quad (19)$$

Substituting (19) for  $C_f$  into (16), we obtain

$$U_e = 3 \text{Re}^{0.125} \sqrt[4]{\frac{\sigma g}{\rho}} \quad (20)$$

Or, in a dimensionless form

$$WeFr = 81 \text{Re}^{0.5} \quad (21)$$

where  $We = \rho \frac{U_e^2 d_p}{\sigma}$  ;

$$Fr = \frac{U_e^2}{gd_p} ; \quad Re = \frac{\rho U_e d_p}{\mu} .$$

The Weber, Froude, and Reynolds numbers are composed according to the critical velocity of the start of air entrainment  $U_e$  and jet diameter at the interaction point  $d_p$  [9]. This means that formula (21) shouldn't contain Froude criteria since the impact of gravitational force is already considered by reducing parameters  $U_e$  and  $d_p$  to their interaction point.

Thus, the obtained as a result of calculations approximate formula (21) differs in its structure from the relationships proposed by other authors [10, 11].

### 3 Results

The obtained calculated correlation is quite coherent with the measurement data of various authors in terms of the degree of impact of individual parameters on the value of the critical velocity of air entrainment  $U_e$  within the range of Reynolds number  $2000 < Re < 15000$ . It can be accounted for by a series of assumptions taken into consideration during the construction of the physical model of the start of air entrainment by turbulent jets, i.e., its imperfection.

## Discussion

We assume that, in the limiting state, the meniscus size before the start of air entrainment is small enough for the weight of the meniscus to be neglected. Now the equilibrium condition for forces in projection on the vertical axis takes the form

$$F_{\tau} - F_{\sigma z} = 0 \quad (22)$$

Otherwise, in stresses, according to (6)

$$\tau - \frac{\sigma}{R} = 0 \quad (23)$$

Considering that tangential shear stresses induced by friction can be described as

$$\tau = C_f \rho \frac{U^2}{2} \quad (24)$$

where  $C_f$  is specific friction resistance; therefore, equation (23) becomes

$$C_f \rho \frac{U_e^2}{2} = \frac{\sigma}{R} \quad (25)$$

The size of the meniscus decreases with increasing jet velocity, as, therefore, does the radius of curvature  $R$ . Suppose that the radius is  $R = kd$ , where  $d$  is jet diameter,  $k$  is proportionality factor; then we can calculate from (25) that

$$U_e = \sqrt{\frac{2}{C_f}} \sqrt{\frac{\sigma}{k\rho d}} \quad (26)$$

For a turbulent flow in a smooth zone, the resistance  $C_f = 0.079 Re^{-0.25}$  [9] and correlation (28) transforms into a dimensionless form

$$We = k_1 Re^{0.25} \quad (27)$$

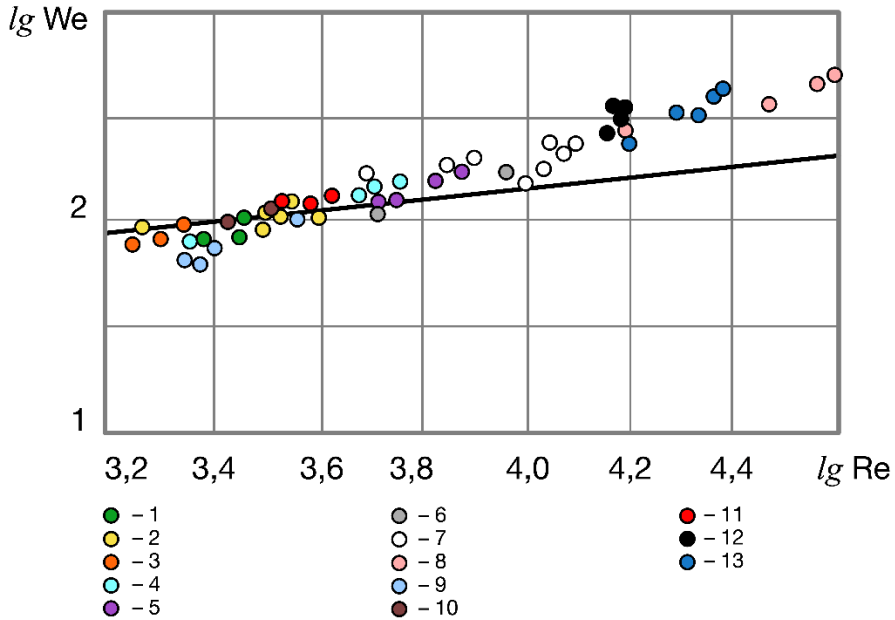


**FIGURE 3.** The results of measurements of various authors for the critical velocity of the start of air entrainment by turbulent jets and the curvature formed according to the calculated correlation. 1-11 – groups of experiments with different values of numbers Fr, Re, We, L/d

Figure 3 shows the results of measurements of various authors [7] for the critical velocity of the start of air entrainment by turbulent jets and the curvature formed according to the calculated correlation (27). Data on fig. 3 was used to determine the coefficient  $k_1$  in (27), which becomes

$$We = 13.3 Re^{0.25} \tag{28}$$

## 4 Conclusion

The study of processes of air entrainment by water jets falling into a liquid allowed us to calculate the minimum velocity of the beginning of air entrainment  $U_c$  by a turbulent free jet when it falls on the surface of a quiescent liquid. The criterion relationship (28), obtained from schematization of air entrainment by turbulent jets flowing from long smooth nozzles, shows a satisfactory agreement with experiments. The criterion relation shows that the jet entrainment rate depends on the Reynolds, Weber, and Froude criteria. Further work should evaluate the contribution of each of the criteria in more detail, evaluate the air entrainment capacity of the jet when the initial flowing conditions change, and conduct further studies of the physical processes that cause the meniscus formation.

## References

1. Jiemin Zhan, Jianbo Zhang, Ye-jun Gong, “Numerical investigation of air-entrainment in skimming flow over stepped spillways,” in Theoretical and Applied Mechanics Letters **6**, p.3 (2016).

2. A. Baylar, M. E. Emiroglu, "Air entrainment and oxygen transfer in a venturi," in Proceedings of the Institution of Civil Engineers: Water and Maritime Engineering, **156**(3), (2003)
3. E. Sande. "Air entrainment by plunging water jets" in I Ph. D. Thesis. (Delft, 1974)
4. M. Yamamura, S. Suematsu, T. Kajiwara, K. Adachi, "Experimental investigation of air entrainment in a vertical liquid jet flowing down onto a rotating roll," in Chemical Engineering Science, **55**(5) (2000)
5. R. Erfanian, M. Moghiman. Experimental investigation of critical air entrainment in ventilated cavitating flow for a forward-facing model," in Applied Ocean Research, **97** (2020)
6. Hojjat Majidi, C. Beckermann, "Modelling of air entrainment during pouring of metal castings," in International Journal of Cast Metals Research, **30**(5) (2017)
7. Y.M. Fetisov. Experimental investigations of the conditions of the onset of air entrainment by plunging liquid jets," in Hydrotechnical Construction **30**, pp.87-91 (1996), <https://doi.org/10.1007/BF02446392>
8. V. Borovkov, Yu. Bryanskaya, Yu. Fetisov and A. Ostyakova, "Capture of Air by a Water Stream at Coupling of Sites of a Non-Pressure Collector with a Large Level Difference. In MATEC web conf., **117** (2017)
9. A.M. Cervantes-Álvarez, A. Sauret, F. Pacheco-Vázquez, "Air entrainment and granular bubbles produced by an impinging jet of grains into water" in arXiv (2019).
10. A.T. Sheridan "Surface entrainment of air by a water jet" in Nature, **209** N5025 pp. 799-800. (1966)
11. T. Lin, H.G. Donnelly, "Gas Bubble entrainment by plunging Laminar Liquid Jets" in AYChEX, **12**(3), (1966)
12. N. Bertola, H. Wang, H. Chanson, "A physical study of air–water flow in planar plunging water jet with large inflow distance" in International Journal of Multiphase Flow, **100**, (2018)
13. P. D. Cummings, H. Chanson, "An experimental study of individual air bubble entrainment at a planar plunging jet," in Chemical Engineering Research and Design, **77**(2) (1999).
14. J. Ma, A. A. Oberai, D. A. Drew, R. T. Lahey, F. J. Moraga, "A quantitative sub-grid air entrainment model for bubbly flows - plunging jets" in Computers and Fluids, **39**(1) (2010)
15. V. Ageorges, J. Peixinho, G. Perret, "Flow and air-entrainment around partially submerged vertical cylinders," in Physical Review Fluids, **4**(6), 2019.
16. A. M. Cervantes-Álvarez, Y. Y. Escobar-Ortega, F. Pacheco-Vázquez, "Air entrainment and granular bubbles generated by a jet of grains entering water," in Journal of Colloid and Interface Science, **574** (2020).
17. R. G. Ramirez de la Torre, M. Kuchta, A. Jensen, "Experiments on air entrainment produced by a circular free-falling jet," in International Journal of Multiphase Flow, **132** (2020)
18. S. Miwa, T. Moribe, K. Tsutsumi, T. Hibiki, "Experimental investigation of air entrainment by vertical plunging liquid jet," in Chemical Engineering Science, **181** (2018)
19. A. Khayrullina, T. van Hooff, B. Blocken, G. J.F. van Heijst, "PIV measurements of isothermal plane turbulent impinging jets at moderate Reynolds numbers," in Experiments in Fluids, **58**(4) (2017)